ORIGINAL ARTICLE
Iran J Allergy Asthma Immunol
September 2013; 12(3):236-246.

Frequency Analysis of Capnogram Signals to Differentiate Asthmatic and Non-asthmatic Conditions Using Radial Basis Function Neural Networks

Mohsen Kazemi[1], Malarvili Bala Krishnan[1], and Teo Aik Howe[2]

[1] Department of Biotechnology and Medical Engineering, Faculty of Bioscience and Medical Engineering, Universiti Teknologi Malaysia, Malaysia
[2] Emergency Department, Hospital Pulau Pinang, Pinang, Malaysia

Received: 26 September 2012; Received in revised form: 19 November 2012; Accepted: 17 January 2013

ABSTRACT

In this paper, the method of differentiating asthmatic and non-asthmatic patients using the frequency analysis of capnogram signals is presented. Previously, manual study on capnogram signal has been conducted by several researchers. All past researches showed significant correlation between capnogram signals and asthmatic patients. However all of them are just manual study conducted through the conventional time domain method. In this study, the power spectral density (PSD) of capnogram signals is estimated by using Fast Fourier Transform (FFT) and Autoregressive (AR) modelling.

The results show the non-asthmatic capnograms have one component in their PSD estimation, in contrast to asthmatic capnograms that have two components. Furthermore, there is a significant difference between the magnitude of the first component for both asthmatic and non-asthmatic capnograms.

The effectiveness and performance of manipulating the characteristics of the first frequency component, mainly its magnitude and bandwidth, to differentiate between asthmatic and non-asthmatic conditions by means of receiver operating characteristic (ROC) curve analysis and radial basis function (RBF) neural network were shown.

The output of this network is an integer prognostic index from 1 to 10 (depends on the severity of asthma) with an average good detection rate of 95.65% and an error rate of 4.34%. This developed algorithm is aspired to provide a fast and low-cost diagnostic system to help healthcare professional involved in respiratory care as it would be possible to monitor severity of asthma automatically and instantaneously.

Keywords: Asthma; Autoregressive (AR) modeling; Capnogram; Fourier analysis; Radial Basis function (RBF) network

Corresponding Author: Mohsen Kazemi, PhD; Department of Biotechnology and Medical Engineering, Faculty of Bioscience and Medical Engineering, Universiti Teknologi Malaysia, 81310 Skudai, Johor, Malaysia. Tel: (+60 17) 746 5497, Fax: (+60 17) 555 8515, E-mail: mohsenkazemi20@gmail.com

INTRODUCTION

Asthma is a chronic inflammatory disease of the bronchial tubes that occurs in about 3 to 5% of all

Copyright© Autumn 2013, Iran J Allergy Asthma Immunol. All rights reserved.

Published by Tehran University of Medical Sciences (http://ijaai.tums.ac.ir)

people and continues to be a significant cause of morbidity and mortality.[1] Traditionally, peak flow meter and spirometer is used to monitor the asthmatic patients which have lots of limitation. Nowadays, capnography is a new method used to monitor the asthmatic condition.[2] It uses the infrared technology to determine the concentration of carbon dioxide. Capnogram is the graphical display of instantaneous CO_2 concentration (mmHg) versus time (second). It is able to show changes in respiration of the patients. It is taken while the patient is breathing as comfortable as possible without requiring any instructions.[2] Capnography can be used on subjects that are either sleeping or awake, and allows various new applications to be envisaged such as detection of nocturnal attacks, evaluation of the duration of action for bronchodilator drugs, intra- and postoperative monitoring of asthmatic patients, and dynamic bronchial provocation tests, especially in children.

A normal capnogram has four phases and an end-tidal point, as shown in Fig.1. Each phase reflects the process of CO_2 elimination.

The flat phase I (*A*-*B*) represents early exhalation that is relatively CO_2-free. As exhalation continues, alveoli containing CO_2 are increasingly recruited and exhaled with non-CO_2-containing gases. This creates a near-vertical rising phase II (*B*-*C*). Near the termination of normal exhalation is a plateau phase III (*C*-*D*). At the end of the plateau phase is *D*, the point that the measured alveolar CO_2 levels best approximate $PaCO_2$. This sampled CO_2 level is known as $PetCO_2$. As inspiration occurs, a near-vertical rapidly falling phase IV (*D*-*E*) is observed.

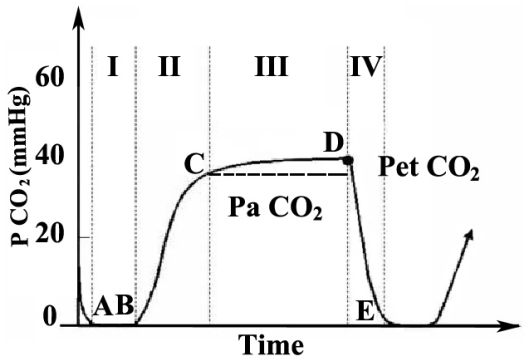

Figure 1. A normal capnogram.

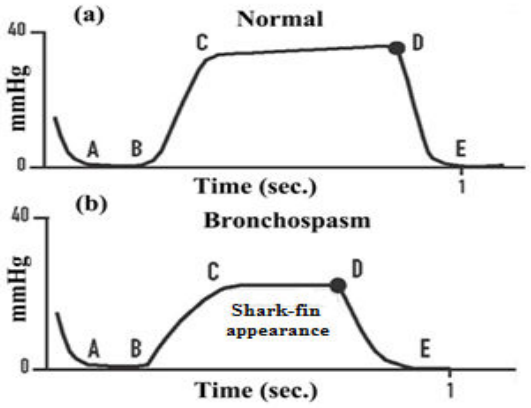

Figure 2. Comparing waveforms: (a) Normal and (b) Bronchospastic.

When ventilation and perfusion are functioning normally, $PetCO_2$ should read 2-5 mmHg higher as compared to $PaCO_2$.[3] A variety of clinical causes can lead to incomplete alveolar voiding.[4]

Therefore, the true end tidal point was never reached. Figure 2 (b) shows the capnogram of an asthmatic patient with an obstruction in tubing and other parts of the breathing circuit. It should be noticed that the ascending limb of the capnogram is prolonged and is not flat, as it should be in normal conditions as shown in Figure 2 (a). These changes give rise to the so called "shark's fin" morphology capnogram in patients with airway obstruction. However, there exists more shape of abnormal capnogram that could be found depending on the patient's condition in.[5]

These variations in capnogram of different diseases cause the researchers carry out analysis of this signal to differentiate between a range of airway illnesses; especially for asthmatic and non-asthmatic conditions.[6-9] However, all these previous studies are manual analysis of capnogram conducted through time domain techniques that is time-consuming and led to erroneous due to human factor such as tiredness and lack of proficiency.

It is important to note that to date, there had been no attempts made to analyze capnogram in frequency domain. Therefore, in this paper, we presented an investigation of the frequency properties of capnogram signals using Fast Fourier Transform (FFT) and Autoregressive (AR) modelling. These methods were used to identify the spectral components of capnogram, and subsequently to differentiate the frequency content of capnogram for different conditions. Essentially, it

helps researchers to understand the nature of capnogram signals and their application to accurately distinguish different types of airway disease.

In this paper, section 2 discusses the methods that consist of data acquisition, preprocessing, FFT analysis, and AR modeling of capnogram signals followed by results and discussion in section 3. Lastly, a conclusion is presented in section 4.

MATERIALS AND METHODS

In this section, 6 sub-steps are presented. The first step is data collection, followed by the pre-processing. In subsection 3, the FFT approach to analyze the frequency component of capnogram signals is presented. Then, the AR modelling method is presented in subsection 4 to estimate the power spectral density of capnogram signals. Lastly, the effectiveness of the extracted features is validated by using receiver operating characteristic (ROC) curve analysis, and radial basis function (RBF) neural networks.

Data Acquisition

The capnogram data were collected from patients with complaints of asthma and breathing difficulties at the Emergency Department of Penang Hospital. First, the capnography sensor was attached on the mouth or nose of the patients. Mainstream capnography method was used in the process of data collection because this method has higher accuracy.[10]

After attaching the sensor on the patient's nose or mouth, the continuous capnogram was recorded using the capnography patient monitor, Capnostream^{TM}20 Model CS08798. The capnogram data in the patient monitor was transferred to a personal computer for analysis. Throughout the study, a total of 23 non-asthmatic capnogram, and 73 asthmatic capnogram were successfully collected. The capnogram for each patient was recorded around five minutes at a sampling frequency of 200Hz. Then, a part of recorded data with the length of five continuous and complete breathing cycles without any artefact (approximately 20 seconds;

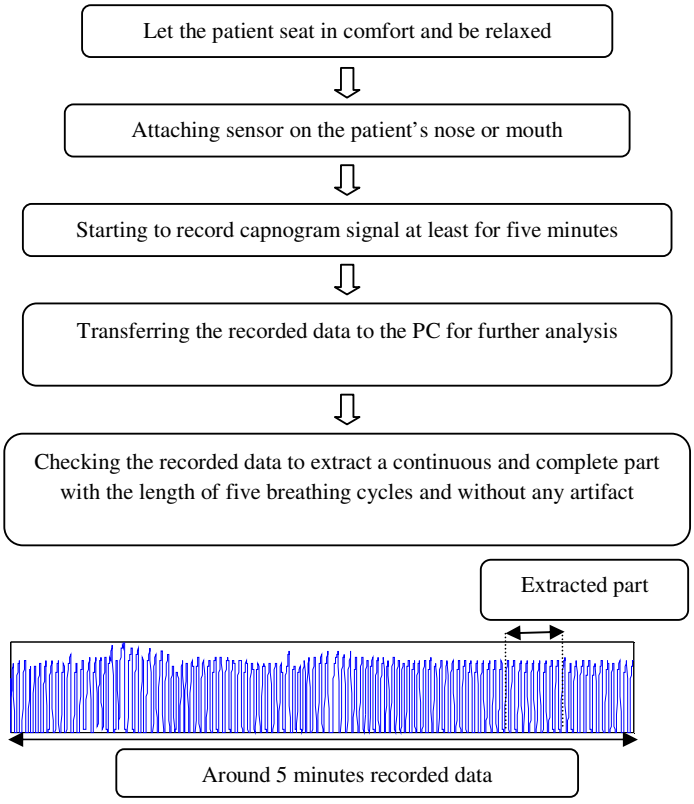

Figure 3. The block diagram of data collection in brief.

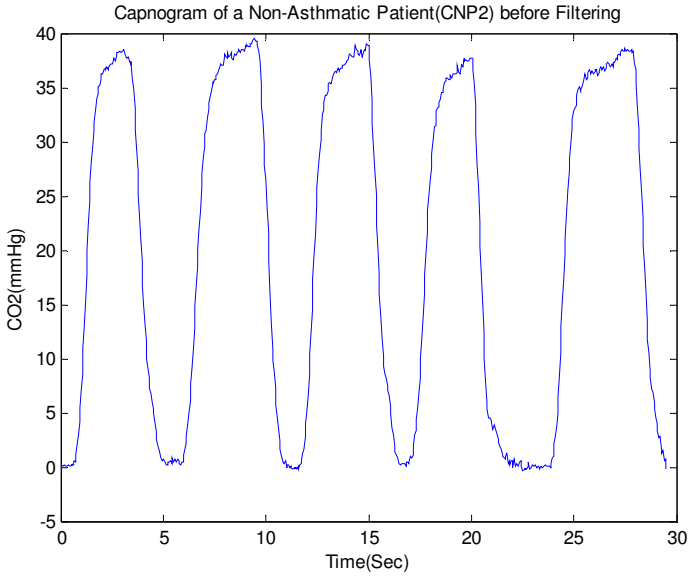

Figure 4. The capnogram signal of CNP2 before filtering.

according to the patient's respiratory rate) was extracted for further analysis. Figure 3 shows the block diagram of data collection in brief In our database, each sample has a designated ID consisting of 3 alphabet letters and a number. The alphabet letter is either CAP (Capnogram of Asthmatic Patient) or CNP (Capnogram of Non-asthmatic Patient) and a number right after the letters which indicates the sample number, e.g. CAP2 represents the second asthmatic sample and CNP6 represents the sixth non-asthmatic sample.

Pre-processing

Data pre-processing was carried out to eliminate unnecessary noise in the recorded capnogram signals. Figure 4 shows a capnogram of non-asthmatic patient (CNP2) before pre-processing.

In this paper, the moving average filtering method was used to smooth the curve due to its simplicity and efficiency, especially for eliminating the high frequency noises within the signals.[11] This method smoothes data by replacing each data point with the average of neighbouring data points defined within a specific span. This process is equivalent to low pass filtering with the response of the smoothing given by the difference equation as follow:

$$y_s(i) = \frac{1}{2N+1}\big(y(i+N) + y(i+N-1) + \cdots + y(i-N)\big) \quad (1)$$

where $y_s(i)$ is the smoothed value for the i[th] data point, *N* is the number of neighbouring data points on either side of $y_s(i)$, and *2N+1* is the *span*. Indeed, the span defines a window that moves across the data set as the smoothed response value is calculated for each predictor value. A large span increases the smoothness but decreases the resolution of the smoothed data set, while a small span decreases the smoothness but increases the resolution of the smoothed data set.[12] The optimal span value depends on the data set and usually requires some trial and error to determine.[13] In this study, we used the span as 13, because it produced the best results for both smoothness and resolution. Furthermore, the correlation coefficients calculated for each signal after filtering justified this span width, e.g. the correlation coefficient for the CNP2 after filtering was 0.9924. Fig.5 shows the non-asthmatic capnogram (CNP2) after smoothing.

FFT Analysis

The discrete Fourier transform (DFT) of an *N*-point sequence *x(n)* is defined as:

$$X(k) = \sum_{n=0}^{N-1} x(n) e^{-j2\pi nk/N} \quad (2)$$

Because *x(n)* may be either real or complex, evaluating *X(k)* requires on the order of *N* complex multiplications and *N* complex additions for each value

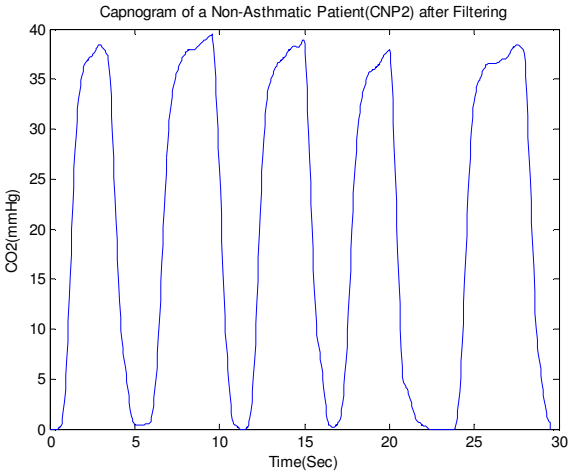

Figure 5. The capnogram signal of CNP2 after filtering.

of *k*. Therefore, because there are *N* values of *X(k)*, computing an *N*-point DFT requires N^2 complex multiplications and additions.

The fast Fourier transform (FFT) is a fast algorithm to compute the DFT which involves decomposing an N-point DFT into successively smaller DFTs.[14]

One of the major applications of the FFT is in analyzing the frequency content of continuous- time signals. In many cases of practical interest, these waveforms are neither periodic nor aperiodic, but a segment of a much longer, and possibly infinite, time series, e.g. EEG, and ECG. Obviously, only a portion of such waveforms can be represented in the finite memory of the computer, and some attention must be paid to how the waveform is truncated, i.e. the need for multiplication of discrete-time signal ($x[n]$) by a window ($w[n]$), as a consequence of the finite-length requirement of the FFT.

Some commonly used windows are Rectangular, Bartlett (triangular), Hanning, Hamming, and Blackman, and all of them have the property that

$$w[n] = \begin{cases} w[M-n] & 0 \le n \le M \\ 0 & Otherwise \end{cases} \qquad (3)$$

In our process, Blackman window with M=256 is selected since the capnogram is biomedical signal related to the respiratory system. So, they are in the category of low frequency signals,[15] and selecting this number as length of window does not affect the time-resolution.

A Blackman window is in the form of:

$$w[n] = \begin{cases} 0.42 - 0.5\cos(2\pi n/M) + 0.08\cos(4\pi n/M) & 0 \le n \le M \\ 0 & Otherwise \end{cases} \qquad (4)$$

One of the advantages of the Blackman window is that it greatly reduced the side-lobes besides a high side-lobe roll-off rate, although the main-lobe's bandwidth has increased, however the extra width is usually worth the trade-off.[16] Also, more information about engineering aspect of window selection could be found at.[17,18]

AR Modeling

Autoregressive (AR) models are widely used for power spectral density (PSD) estimation.[19] The AR model of a time series is represented in the following form:

$$x(n) = -\sum_{m=1}^{p} a(m)x(n-m) + e(n) \qquad (5)$$

Where *x(n)* is the time series, *a(m)* are AR parameters, *p* is the model order, and *e(n)* is the prediction error.

Recently, because of the good performance of AR spectral estimation methods over traditional approaches, these methods have been successfully applied to analyze biomedical signals.[20] A signal spectrum shows how the power is distributed as a function of frequency, and AR spectral analysis can provide the number, centre frequency, and associated power of oscillatory components in a time series.

A variety of AR models are currently used to estimate the PSD of biomedical signals. The Burg method was selected because it estimates the reflection coefficients instead of the prediction coefficients. In comparison with other approaches such as autocorrelation, covariance, modified covariance, and recursive least squares (RLS), this method does not require run-off of the data sequence by zero padding and has minimal phase characteristic with high accuracy.[21] Further mathematical equations behind this method are available at.[22]

One of the crucial parts for the AR method is the selection appropriate value for the model order *P*. In spectral estimation, the accuracy of the estimated spectrum is critically dependent on the model order that is chosen. It means that a too low model order can generate an over smoothed spectrum, whereas too high

a value of order may introduce spurious details such as false peaks into spectrum.[23]

The model order can be estimated using the Akaike information criterion (AIC) which is one of the most popular approaches to determine an optimum model order and minimize the information entropy of the signal identified as follows:

$$AIC(P) = N \ln(E_P) + 2P \quad (6)$$

where E_P, P, and N individually represent the estimation of mean-squared error, the order of the filter, and the number of input signal samples.

In this study, the AIC for different model orders were calculated. As shown by the results in Fig.6, at $P=10$ the AIC value was smallest compared to the other number of P. So, the model order 10 was selected since the minimum of error variance was observed at this value of P.

Performance Measure

The effectiveness of extracted coefficients is assessed by Receiver Operating Characteristic (ROC) curve analysis and two indices included sensitivity and specificity that are often employed in medical applications.[24] The results of a particular test are considered in two categories; one population with a disease, and the other population without the disease. There will be some cases with the disease correctly classified as positive (TP = True Positive fraction), and some cases with the disease will be classified negative (FN = False Negative fraction). On the other hand, some cases without the disease will be correctly classified as negative (TN = True Negative fraction), but some cases without the disease will be classified as positive (FP = False Positive fraction). According to this classification, sensitivity and specificity that estimate the classifier's performance in different classes,[25] define as follow:

$$Sensitivity = \frac{TP}{TP + FN} \quad (7)$$

$$Specificity = \frac{TN}{TN + FP} \quad (8)$$

So, Sensitivity is probability that a test result will be positive when the disease is present, and Specificity is probability that a test result will be negative when the disease is not present.

Furthermore, with ROC curves, when the variable under study cannot distinguish between the two groups, i.e. where there is no difference between the two distributions, the area under the ROC curve (AUC) will be equal to 0.5, whereas when there is a perfect separation of the values of the two groups, i.e. there is no overlapping of the distributions, the AUC equals 1. Also the P-value is the probability that the sample AUC is found when the true population area under the ROC curve is 0.5 (null hypothesis: Area = 0.5). If P is low (P<0.05) then it can be concluded that the area under

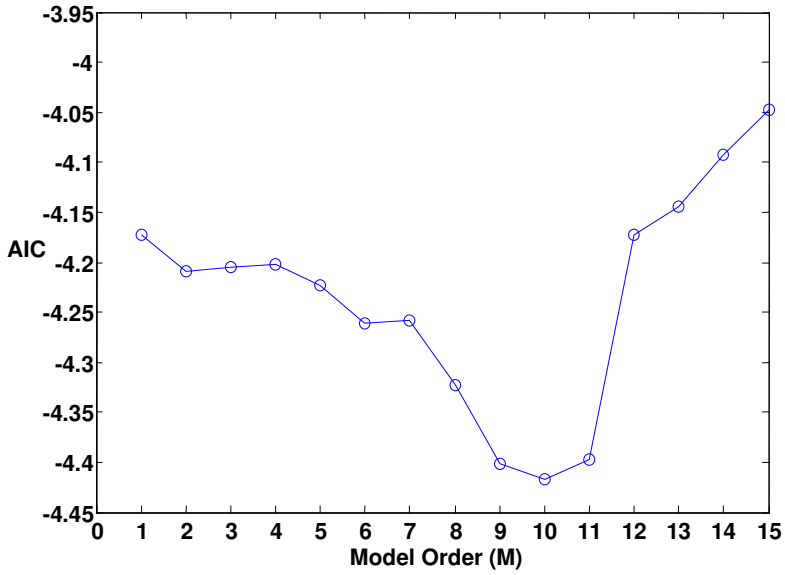

Figure 6. AIC values for different model orders.

the ROC curve is significantly different from 0.5 and that therefore there is evidence that the capnogram test does have an ability to distinguish between the two groups.[26]

RBF Neural Networks

A radial basis function (RBF) neural network is designed to automatically cluster and classify the patients with different asthmatic severity. A radial basis network is a feed-forward neural network using the radial basis activation function. The RBF network generally consists of two weight layers; the hidden layer and the output layer, which can be described as follows:[27]

$$y = w_0 + \sum_{i=1}^{n_h} w_i f(\|\mathrm{x} - c_\mathrm{i}\|) \qquad (9)$$

where f are the radial basis functions, w_i are the output layer weights, w_0 is the output offset, x are inputs to the network, c_i are the centres associated with the basis functions, and n_h is the number of basis functions in the network. Furthermore, the $\|\ .\ \|$ denotes the Euclidean norm that measures the size of the vector in a general sense.

The RBF networks have benefits such as easy design, good generalization, strong tolerance to input noise, and online learning ability.[28] Artificial neural networks have been successfully applied to hosts of pattern recognition and classification tasks, time series prediction, data mining, function approximation, data clustering and filtering, and data compression. It can be used to solve a wide variety of problems while being robust to error in training data. Hence, the developed RBF network will help the medical practitioners and physicians to monitor severity of asthmatic patients.

RESULTS

In this section, the results of applying FFT on capnogram signals and the estimated PSD using AR modeling-Burg method are thoroughly presented and discussed.

FFT Analysis Results

After selecting the appropriate window, the classic FFT algorithm was applied on the capnograms of asthmatic and non-asthmatic patients. Figure 7 and Fig.8 show the FFT of the capnogram of a non-asthmatic patient (CNP2) and the capnogram of an asthmatic patient (CAP9), respectively.

Based on Figure 7 and Fig.8, and the results for all data, there was a significant difference between the number of component and their magnitudes in the FFT of CAPs and CNPs. The number of main-lobe in the asthmatic capnogram was equal to 2 in contrast to non-asthmatic capnogram, which had only 1 main-lobe. Also, the frequency of this components and their related bandwidth were also different in both asthmatic and non-asthmatic samples. For asthmatic patients, the frequency and bandwidth of the first main-lobe were around 0.078 Hz and 0.23 Hz, respectively. Whereas, for non-asthmatic patients these values for only component were around 0.04 Hz and 0.08 Hz, respectively.

Table 1 shows the performance indices of the magnitude, frequency, and bandwidth of the dominant component in the FFT of CNPs, and CAPs.

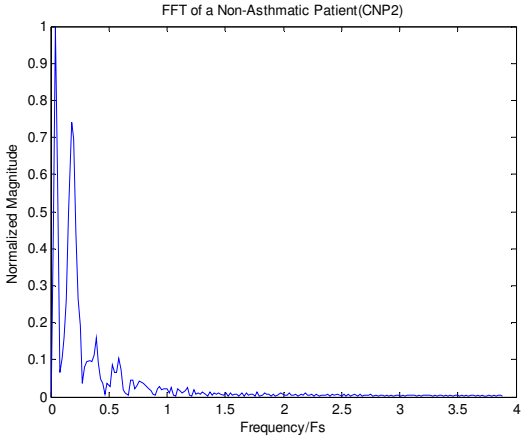

Figure 7. The FFT of a non-asthmatic capnogram (CNP2).

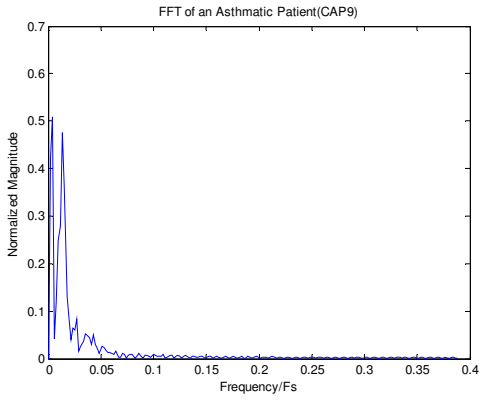

Figure 8. The FFT of an asthmatic capnogram (CAP9).

Copyright© Autumn 2013, Iran J Allergy Asthma Immunol. All rights reserved.

Published by Tehran University of Medical Sciences (http://ijaai.tums.ac.ir)

Based on the Table 1, all features have AUC > 0.8 and p <0.0001. This shows that all features of the dominant peak in the FFT of CAPs and CNPs are feasible to be applied in the differentiation of the asthmatic and non-asthmatic conditions. However, compared to all the features, it can be seen that the bandwidth of the main-lobe and its magnitude have noticeable AUC (with p-value < 0.0001), sensitivity (96.77 and 97.54, respectively) and specificity (94.74 and 94.63, respectively) which is considerably more efficient to classify the capnogram data in two groups, and further differentiate the asthmatic conditions.

AR Modeling-Burg Method Results

Figure 9 and Figure 10 show the PSD estimation of a non-asthmatic capnogram (CNP2) and an asthmatic capnogram (CAP9) by using Burg method of AR modeling

As Figure 9 and Figure 10 show, and according to the results for all data, the PSD estimation of the non-asthmatic capnogram signals (CNPs) consists of one component, while for asthmatic capnogram signals (CAPs), this estimation produced two components. Hence by using the second component in PSD estimation using Burg method, asthmatic and non-asthmatic conditions can be differentiated without errors. The frequency of the first component, and the total power of the PSD estimation for asthmatic capnogram were around 0.02 Hz and 0.195, respectively, whereas, these values for non-asthmatic capnogram were around 0.011 Hz and 0.354, respectively.

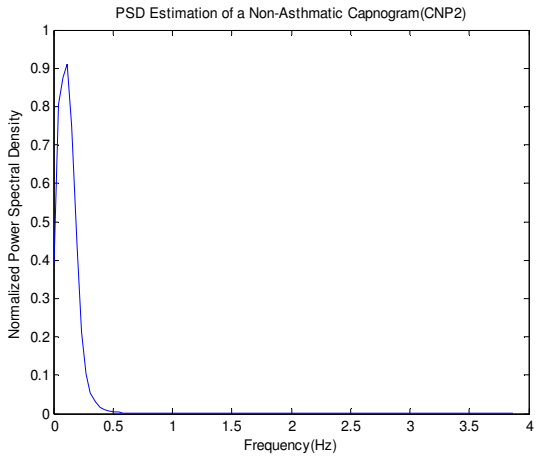

Figure 9. Power spectral density of a non-asthmatic capnogram (CNP2).

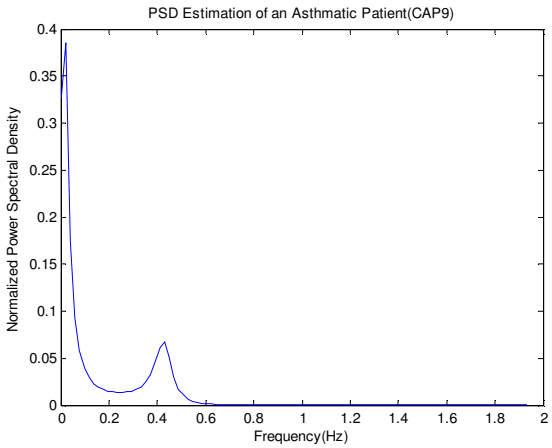

Figure 10. Power spectral density of an asthmatic capnogram (CAP9).

Table 2 shows performance indices for the frequency of the first component and the total power in the PSD estimation of the CAPs and CNPs.

According to the Table 2, both frequency of the first component and the total power in the PSD estimation had AUC>0.7 and p<0.003. This indicated that all features in the PSD distribution of CAPs and CNPs were functional in differentiating the asthmatic and non-asthmatic conditions. However, it is obvious that the first component frequency has noticeable AUC and p<0.0001, accompanied by high sensitivity and specificity, which is efficient to classify the capnogram signals in two groups. As a result, this parameter and the frequency of the second component (that only exist in PSD of asthmatic patients) can significantly differentiate the asthmatic conditions.

Features Effectiveness using RBF Neural Network

According to results obtained, our feature vector consists of four elements. These are the number of frequency components, magnitude and frequency of the first component, and frequency of the second component in PSD estimation.

First of all, two different databases were created in which one of them was used for training process and the other one was used as the test data. The bottom line is that, the training database had one additional element in feature vector which was medical practitioner diagnosis of asthmatic severity. It is represented by a number from one to ten for a non-asthmatic patient to a patient, who suffers from very severe asthma, respectively, that is the main goal of this research.

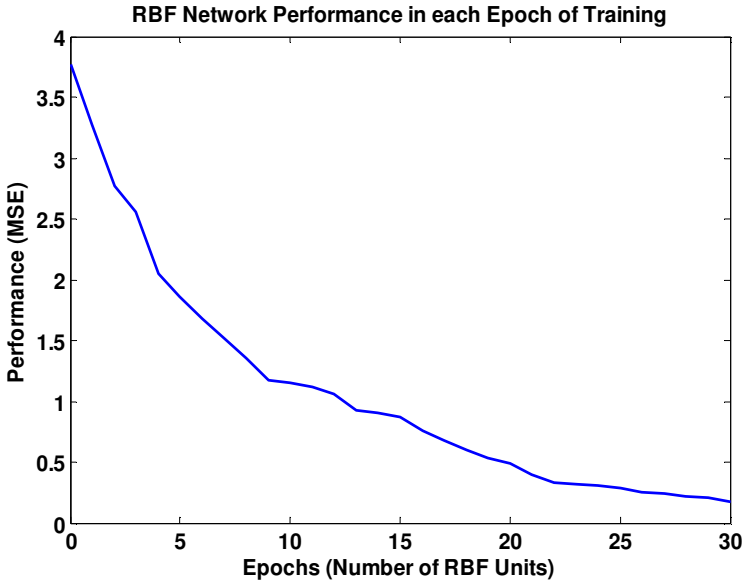

Figure 11. The performance of designed RBF neural network.

Table 1. AUC and p-value of the magnitude, frequency, and bandwidth of the main-lobe in the FFT of CNPs, and CAPs.

Performance index	Magnitude of the main-lobe (Normalized)	Frequency of the main-lobe (Hz)	Bandwidth of the main-lobe (Hz)
Sensitivity	97.54	80.65	96.77
Specificity	94.63	82.11	94.74
AUC	0.937	0.847	0.975
P-Value	<0.0001	<0.0001	<0.0001

Table 2. AUC and p-value for the frequency of the first component and total power in the PSD estimation of CNPs, and CAPs.

Performance index	Frequency of the First Component (Hz)	Total Power
Sensitivity	98.23	83.87
Specificity	95.08	84.21
AUC	0.996	0.722
P-Value	<0.0001	0.0023

The process of training will be stopped when the number of RBF units is equal to thirty, or the program will reach the mean squared error (MSE). This limit for RBF units was selected in order to get the best and most accurate results from the designed RBF neural network for this study. Figure 11 shows the performance of neural networks in each training epoch.

As shown in Figure 11, after thirty training epochs, the RBF network reached the desire MSE. After training the RBF network, the test database was loaded

into the RBF networks. According to the results, the output of this network is an integer prognostic index from 1 to 10 (depends on the severity of asthma; 1 is stand for healthy people, and 10 is for too severe asthma) with an average good detection rate of 95.65% and an error rate of 4.34%. Consequently, the defined index could be used in capnography to detect the severity of asthma in patient with respiratory difficulties with good accuracy and also as an online system.

DISCUSSION

Capnogram is a vital representation of the respiratory system. Therefore, the analysis of this physiological signal could lead to the development of a computerized method to differentiate airway disorders, which could benefit the heathcare professional involved in respiratory care. Previous studies conducted for capnogram signal analysis used only conventional time domain methods. In this paper, for the first time, frequency contents of capnogram signals have been investigated. The results showed that by using these properties, asthmatic and non-asthmatic conditions can be perfectly differentiated. Also, by the incorporation of a RBF neural network, the severity of asthma in patient could be automatically assessed as an index in capnographs. This method is an innovative idea that could further assists the healthcare professionals and medical practitioners involved in respiratory care as it would be possible to monitor severity of asthma automatically and instantaneously with minimum human errors.

ACKNOWLEDGEMENTS

This study was conducted as a part of the fundamental research grant scheme, supported by the Ministry of Higher Education Malaysia. The authors gratefully acknowledge the Universiti Teknologi Malaysia (UTM) for providing facilities and laboratory equipments.

REFERENCES

1. Steven E. Weinberger, Barbara A. Cockrill, Jess Mandel, Principles of pulmonary medicine, 5th Ed., Elsevier Inc., 2008.
2. Rhoades C, Thomas F. Capnography: beyond the numbers. Air Med J 2002; 21(2):43-8.
3. Giner J, Casan P. Pulse Oximetry and Capnography in Lung Function Laboratories. Arch Bronconeumol 2004; 40(7):311-4.
4. Thompson JE, Jaffe MB. Capnography waveforms in the mechanically ventilated patient. Respir Care 2005; 50(1):100-9.
5. Smalhout B., Kalenda Z., An Atlas of Capnography, 2nd Ed., Kerckebosche Zeist Press, 1981.
6. You B, Peslin R, Duvivier C, Vu V, Grilliat JP. Expiratory capnography in asthma. Eur Respir J 1994: 7(2):318-23.
7. Yaron M, Padyk P, Hutsinpiller M, Cairns CB. Utility of the expiratory capnogram in the assessment of bronchospasm. Ann Emerg Med 1996; 28(4):403-7.
8. Druck J, Rubio PM, Valley MA, Jaffe MB, Yaron M. Evaluation of the slope of phase III from the volumetric capnogram as a non-effort dependent in acute asthma exacerbation. Annual of Emergency Medicine 2007; 50(3):130-6.
9. Tan Teik Kean, M. B. Malarvili. Analysis of capnography for asthmatic patient, IEEE International Conference on Signal and Image Processing Applications 2009, 464-7.
10. Swenson J, Henao-Guerrero PN, Carpenter JW. Clinical Technique: Use of Capnography in Small Mammal Anesthesia. Journal of Exotic Pet Medicine 2008: 17(3):175-80.
11. Kirkko-Jaakkola M, Collin J, Takala J. Bias Prediction for MEMS Gyroscopes, IEEE Sensors 2012; 12(6):2157-63.
12. Facchinetti A, Sparacino G, Cobelli C. An Online Self-Tunable Method to Denoise CGM Sensor Data. IEEE Trans Biomed Eng 2010: 57(3):634-41.
13. Gonzalo R. Arce, Nonlinear Signal Processing; A Statistical Approach, John Wiley & Sons, Inc., New Jersey, 2005.
14. Gao S, Mateer T. Additive Fast Fourier Transforms Over Finite Fields. IEEE Transactions on Information Theory 2010; 56(12):6265-72.
15. Lauralee Sherwood. Fundamentals of Physiology: A Human Perspective, Thomson Brooks and Cole Inc., 2006.
16. Soni RK, Jain A, Saxena R. An improved and simplified design of Pseudo-transmultiplexer using Blackman window family. Digital Signal Processing 2010; 20(3):743-9.
17. John L. Semmlow, Biosignal and Biomedical Image Processing, Marcel Dekker Inc., 2004.
18. Alan V. Oppenhein, Ronald W. Schafer, Discrete-Time

Signal Processing, Prentice Hall Signal Processing Series, 3rd Ed., 2010.

19. Hsu HW, Liu CM. Autoregressive Modeling of Temporal/Spectral Envelopes With Finite-Length Discrete Trigonometric Transforms. IEEE Transactions on Signal Processing 2010; 58(7):3692-705.
20. Takalo RH, Ihalainen HH. Tutorial on Univariate Autoregressive Spectral Analysis Export. J Clin Monit Comput 2006; 20:379-88.
21. Tracey Cassar, Kenneth P. Camilleri, Simon G. Fabri, Order Estimation of Multivariate ARMA Models. IEEE journal of Selected Topics in Signal Processing 2010; 4(3):494-503.
22. K J Blinowska, J Zygierewicz, Practical Biomedical Signal Analysis, Poland, CRC Press (Taylor & Francis Group, LLC), 2011.
23. Fang-Xiang Wu, Wen-Jun Zhang, Dynamic-Model-Based Method for Selecting Significantly Expressed Genes From Time-Course Expression Profiles. IEEE Trans Inform Technol Biomed 2010; 14(1):16-22.
24. Temko A, Lightbody G, Thomas EM, Boylan GB, Marnane W. Instantaneous Measure of EEG Channel Importance for Improved Patient-Adaptive Neonatal Seizure Detection. IEEE Trans Biomed Eng 2012; 59(3):717-27.
25. Ramachandran P, Lu WS, Antoniou A. Filter-Based Methodology for the Location of Hot Spots in Proteins and Exons in DNA. IEEE Biomed Eng 2012; 59(6):1598-1609.
26. Acharya UR, Dua S, Du X, Sree S V, Chua CK. Automatic Diagnosis of Glaucoma Using Texture and Higher Order Spectra Features. IEEE Trans Inf Technol Biomed 2011; 15(3):449-55.
27. M. D. Buhmann, Radial Basis Functions: Theory and Implementations, Cambridge University Press, Cambridge, 2004.
28. Tiantian Xie, Hao Yu, Joel Hewlett, Pawel Rozycki, Bogdan Wilamowski. Fast and Efficient Second-order Method for Training Radial Basis Function Networks. IEEE Transactions on Neural Networks and Learning Systems 2012; 23(4):609-19.